Manoj Kr. Deka and Apul N. Dev*

Solitary Wave with Quantisation of Electron's Orbit in a Magnetised Plasma in the Presence of Heavy Negative Ions

https://doi.org/10.1515/zna-2019-0296
Received August 7, 2019; accepted December 20, 2019

Abstract: The propagation characteristics of solitary wave in a degenerate plasma in the presence of Landau-quantised magnetic field and heavy negative ion are studied. The nature of solitary wave in such plasma under the influence of magnetic quantisation and the concentration of both electrons and negative ions, as well as in the presence of degenerate temperature, are studied with the help of a time-independent analytical scheme of the solution of Zakharov–Kuznetsov equation. The electron density, as well as the magnetic quantisation parameter, has an outstanding effect on the features of solitary wave proliferation in such plasma. Interestingly, for any fixed electron density, the magnetic quantisation parameter has an equal control on the maximum height and dispersive properties of the solitary wave. Toward higher temperatures and higher magnetic fields, the width of the solitary wave decreases. For a lower magnetic field, the maximum amplitude of the solitary wave decreases rapidly at higher values of degenerate temperature and negative ion concentration; however, at a lower value of degenerate temperature, the maximum amplitude increases with increasing negative ion concentration.

Keywords: Degenerate Trapped Electrons; Magnetised Plasma; Negative Ions; Zakharov–Kuznetsov Equation.

1 Introduction

Degenerate plasmas containing positive and negative ions, especially pair-ion or multi-ion plasmas, have been getting enormous importance in studying the localised electrostatic oscillations in space astrophysical as well as laboratory plasma environment. The presence of negative ions in different ionospheric layers [1], cometary environment [2], and plasma reactors [3], as well as in laboratory experiments [4], has been well studied. Investigations on solitary waves in electron-ion and multispecies plasma in degenerate/nondegenerate, as well as in relativistic/ultrarelativistic plasmas, have been widely carried out because of its occurrence and importance in different plasma environment [5–11]. Apart from these observations, electrostatic solitary wave in magnetised plasma environment considering different distribution of electron such as nonthermal distribution, kappa distribution, and so on, which is relevant from the space plasma point of view, has been well explored [12–19]. On the other hand, in the presence of higher magnetic field, if the cyclotron frequency exceeds the typical Coulomb energy, then the atoms or molecules are significantly affected. In quantum plasmas, in the presence of higher magnetic field, the cyclotron orbits of electrons are quantised [20], and due to this, the occupancy of electrons occurs in discrete Landau levels where in each level the number of electrons is directly proportional to the strength of the magnetic field, which is popularly known as Landau quantisation. As the magnetic field increases, more and more electrons can be accommodated in each Landau level. Thus, the entire electronic properties simply become a function of the strength of the applied magnetic field. Now, based on the astrophysical data, the surface magnetic field of a neutron star is $B \approx 10^{11} - 10^{12} G$, and the internal field can reach $B \approx 10^{15} G$ or even higher [21–27]. In such strong magnetic fields, it is expected that the thermodynamic properties and wave dynamics in degenerate plasmas would be quite different, as the characteristic energy of electron on a Landau level reaches the nonrelativistic limit of the electron chemical potential $\mu = \varepsilon_{Fe} = \hbar|e|B/2m_e c$, where $B = B_s v_F^2/c^2$ with $B_s = m_e^2 c^3/|e|\hbar$, $v_F = p_{Fe}/m_e$, is the velocity of the electrons on the Fermi surface; $n_{e0} = p_{Fe}^3/3\pi^2\hbar^3$ is the equilibrium number density; p_{Fe} is the momentum on the Fermi surface; here, symbols have their usual meaning. On the other hand, degenerate plasma has a wide application such as metallic

***Corresponding author: Apul N. Dev,** Center for Applied Mathematics and Computing, Siksha 'O' Anusandhan (Deemed to be University), Bhubaneswar 751030, Odisha, India, E-mail: apulnarayan@gmail.com, apulnarayandev@soa.ac.in
Manoj Kr. Deka: Department of Applied Sciences, Gauhati University, Guwahati 781014, Assam, India

and semiconductor nanostructures, which include metallic nanoparticles, metal clusters, thin-film spintronics, nanotubes, quantum wells and quantum dots, nanoplasmonic devices, quantum x-ray free electron lasers, high-energy density physics especially inertial confinement physics, and so on, where such plasma conditions are prevalent [28–31]. Even hole acoustic waves along with instability in semiconductor plasma in the presence of Landau quantisation are reported to have its existence in degenerate regime [32]. Apart from these, in the next-generation intense laser–solid density plasma interaction experiments, magnetic field of the order of giga-Gauss appears in the petawatt lasers, and the strong Landau quantisation can happen in such range of magnetic field [33, 34]. On the other hand, apart from the presence of negative ions in the plasma environment mentioned above [1–4], very recently, Mondal et al. reported the existence of negative ions in the diagnostics of laser-induced plasma in petawatt range, although their magnetic field was a bit low [35]. Perhaps, in the future, such type of experiment may come up with stronger magnetic field. Thus, we see that these types of plasma environment have a wide application from laboratory to extreme space plasma environment.

There have been a few investigations on the propagation of large-/small-amplitude solitary wave in the presence of Landau-quantised magnetic field where the effect of such high magnetic field on the amplitude/width of the solitary wave in relativistic/nonrelativistic plasma regime has been successfully shown [36–39]. On the other hand, Recently, Hossen et al. [40], in a magnetised degenerate plasma, observed the unique effect of oblique magnetic field on the switching between compression and rarefaction of the solitary wave. Mahmood et al. [41] observed the effect of charged state of helium positive ions on the Mach number of the compressive solitons in a quantum plasma and concluded that in case of doubly charged positive ions subsonic and supersonic compressive solitons are possible, whereas in case of singly charged positive ions only subsonic compressive solitons are possible. El-Shamy et al. [42] reported that the ion's cyclotron frequency and wave vector direction have a dominating effect on the propagation of solitary wave in a degenerate magnetised plasma. Masud and Mamun in a report, described that the height of solitary wave in a degenerate dense plasma depends strongly on normalised number density of electron to positive ion [43]. In another report, Ghosh [44] analysed the properties of nonlinear waves of low frequency in a dissipative degenerate plasma where he reported that the source of dissipation was ion-neutral collision. Also, he reported that such weak dissipative soliton exists only if the ion-neutral collision rate is low enough compared to ion plasma frequency. Haas and Mahmood [45] carried out a study on the effect of arbitrary degeneracy on the propagation of ion acoustic soliton and concluded that in plasma with a relatively low density only compressive-type solitary structure appears, whereas in dense plasma, both compressive- and rarefactive-type solitary structures appear. Sahu [46], in his report, numerically confirmed that solitary wave's amplitude increases with increasing time in cylindrical as well as spherical geometry and also found that the cylindrical solitons are slow compared to spherical soliton. He also reported that dissipation occurred due to the collisional effects in the plasma system, and the quantum Bohm potential can further enhance this dissipation of the plasma system.

Hossen and Mamun [47] in a report investigated the properties of solitary wave in a multispecies degenerate plasma and confirmed that basic characteristics of modified ion acoustic waves are greatly modified by the presence of different charged state of heavy ions. Hussain et al. [48] reported the features of solitary wave propagation in nonplanar geometry in degenerate negative ion plasma and found that quantum diffraction parameter, positive/negative ion temperature, and degenerate electron density have a patent effect on the phase velocity and the structure of the soliton. Hussain and Akhtar [49] studied the collisional effect in negative ion quantum plasma and observed a kind of damped K-dV solitary wave where the amplitude (width) decreases (increases) with increasing collisional frequency, and also, they found that the tunnelling effect of degenerate electrons has a significant effect on the width of the solitary structure in such collisional plasma. Tie-Lu et al. [50] studied the modulation instability of solitary waves in a degenerate negative ion plasma and concluded that the temperature and density ratio of negative to positive ions, as well as degeneracy effect, have a strong control of the instability regions both in the weakly and ultrarelativistic limit. Sahu et al. [51] discussed the role of quantum diffraction parameter, positive ion–to–negative ion density ratio, and Mach number on the ion acoustic wave in a degenerate plasma and reported that these parameters can modify the basic properties of solitary wave. They also found that chaotic as well as quasi-periodic oscillation can coexist in such plasma, and the nonlinear ion acoustic wave can switch from quasi-periodic to chaotic, depending on Mach number or quantum diffraction parameter H. Here, we have tried to summarise the outstanding behaviour of solitary waves in a Landau-quantised degenerate dense plasma in the presence of heavy static negative ion through a Zakharov–Kuznetsov (Z–K) equation, which we believe has not yet

been addressed. We expect the results summarised here can be important in case of space and laboratory plasma.

2 Theoretical Formulations

In order to study the features of ion acoustic waves in a degenerate plasma with electrons following the orbits of a quantised magnetic field, the basic set of equations can be written as follows [6, 36, 39, 52–57]:

$$\frac{\partial n_i}{\partial t} + \boldsymbol{\nabla}.(n_i \boldsymbol{v}_i) = 0 \tag{1}$$

$$\frac{\partial \boldsymbol{v}_i}{\partial t} + (\boldsymbol{v}_i.\boldsymbol{\nabla})\boldsymbol{v}_i = \frac{q_i}{m_i}(-\nabla\varphi + \boldsymbol{v}_i \times \boldsymbol{B}_0/c) \tag{2}$$

$$\nabla^2\varphi = 4\pi e(n_e - n_i + Z_h n_{ho}) \tag{3}$$

Now, following the Fermi–Dirac statistics, the electron occupancy in energy range ε and $\varepsilon + d\varepsilon$, in presence of quantised magnetic field, can be written as follows [46, 52]:

$$n_e = \frac{p_{Fe}^2\eta}{2\pi^2\hbar^3}\sqrt{\frac{m_e}{2}}\sum_{l=0}^{\infty}\int_0^{\infty}\frac{\varepsilon^{-1/2}}{1+\exp\big((\varepsilon - U)/T'\big)}\,\mathrm{d}\varepsilon \tag{4}$$

where $U = e\,\varphi + \mu - l\,\hbar\,\omega_{c\,e}$ with potential function and minus is the chemical potential and $\eta = \hbar\omega_{ce}/\varepsilon_{Fe}$, the effect of quantising magnetic field appears through η, the cyclotron frequency of the electron is given by $\omega_{ce} = eB_0/m_e c$, $\varepsilon_{Fe} = \left(\hbar^2/2m_e\right)\left(3\pi^2 n_{e0}\right)^{2/3}$ is the electron Fermi energy, and $n_{e0}\left(= p_{Fe}^3/3\pi^2\hbar^3\right)$ is the equilibrium electron density. The chemical potential is not truly equal to the Fermi energy when $T' \neq 0$; however, in the case when $T'/\varepsilon_{Fe} \leq 1$, it is reasonable to take $\mu = \varepsilon_{Fe}$. The potential φ and temperature T are normalised in the following manner: $\phi = \varphi e/\varepsilon_{Fe}$ and $T = \left(\pi T'/2\sqrt{2}\varepsilon_{Fe}\right)$, respectively. The summation above is over all the Landau levels, and we note here $l = 0$ refers to the case without a quantising magnetic field. Now, from basic quantum mechanics of macroscopic system, we know that there is an extremely high density of energy levels in the energy eigenvalue spectrum. The number of levels in a finite range of energy spectrum increases exponentially with number of particles (N) in the system, and the separation between the levels is proportional to $10^{-\mathrm{N}}$ [58, 59]. Therefore, we can conclude that it is reasonable to take a continuous energy spectrum instead of a discrete one. Thus, to obtain an expression of the density $\mathrm{n_e}$ after integration, we can separate the $l = 0$ case from the summation and replace the summation in (4) by integration, which is obtained from the condition that the integrand must remain a real quantity; we derive the expression for electron density as follows (for details of derivation of electron density expression, see Appendix):

$$n_e = n_{e0}\left\{\frac{3}{2}\eta(1+\phi)^{\frac{1}{2}} + (1+\phi-\eta)^{\frac{3}{2}} - \frac{\eta T^2}{2}(1+\phi)^{-\frac{3}{2}} + T^2(1+\phi-\eta)^{-\frac{1}{2}}\right\} \tag{5}$$

which on expanding (5) becomes

$$\begin{aligned}\frac{n_e}{n_{e0}} &= N_e \\ &= \frac{\eta}{2}\left(3 - T^2\right) + (1-\eta)^{\frac{3}{2}} + T^2(1-\eta)^{-\frac{1}{2}} \\ &\quad + \frac{3\phi}{2}\left\{\frac{\eta}{2}\left(1 + T^2\right) + (1-\eta)^{\frac{1}{2}} - \frac{T^2}{3}(1-\eta)^{-\frac{3}{2}}\right\} \\ &\quad + \frac{3\phi^2}{8}\left\{-\frac{\eta}{2}\left(1 + 5T^2\right) + (1-\eta)^{-\frac{1}{2}} \right. \\ &\quad \left. + T^2(1-\eta)^{-\frac{5}{2}}\right\}\end{aligned} \tag{6}$$

The charge neutrality condition is given by $n_{eo} + Z_h n_{no} = n_{io}$, where n_{i0}, n_{eo}, n_{hno} are the number density for ions, electron, and heavy negative ion respectively. Now, we can find the normalised equations from (1) to (3),

$$\frac{\partial N_i}{\partial \bar{t}} + \nabla(N_i V_i) = 0 \tag{7}$$

$$\frac{\partial V_i}{\partial \bar{t}} + (V_i\nabla)V_i = -\nabla\phi + V_i\Omega_i \tag{8}$$

$$\nabla^2\phi = (\mu_e N_e - N_i + \mu_{hn}) \tag{9}$$

where $\Omega_i = \omega_{ci}/\omega_i$, $\mu_e = n_{e0}/n_{i0}$ is the electron–to–ion density ratio, and $\mu_{hn} = Z_h n_{hn0}/n_{i0}$ is the heavy negative ion–to–ion density ratio; Z_h is the charged state of heavy negative ions, and $\omega_{ci} = eB_0/m_i c$ is the ion cyclotron frequency. The above equations are normalised with the following normalised parameters: length (x, y, and z) by Debye lengths $\lambda_{Fe} = \left(\varepsilon_{Fe}/4\pi n_{i0}e^2\right)^{1/2}$; the velocity ($v$) is normalised by Fermi ion sound velocity $C_s = (\varepsilon_{Fe}/m_i)^{1/2}$; the time ($t$) is normalised by the inverse of ion plasma frequency $\omega_i^{-1} = \left(4\pi n_{i0}e^2/m_i\right)^{-1/2}$, and ion density n_i is normalised by equilibrium density n_{i0}.

3 Evolution Equation of Nonlinear Wave

Adopting the standard reductive perturbation technique and using the following stretched coordinates, we derive

the evolution equation of solitary wave in terms that the Z–K equation is

$$\xi = \varepsilon^{1/2}(X - \lambda\bar{t}), \quad \eta = \varepsilon^{1/2}Y, \\ \zeta = \varepsilon^{1/2}Z, \quad \text{and} \quad \tau = \varepsilon^{3/2}\bar{t} \tag{10}$$

where λ is the normalised phase speed. The dependent parameters such as ion density (N_i), velocity of the ions in three different directions ($V_{ix,iy,iz}$), and potential ϕ are expanded in a power series in terms of the expansion parameter ε as

$$\left.\begin{aligned} N_i &= 1 + \varepsilon N_i^{(1)} + \varepsilon^2 N_i^{(2)} + \varepsilon^3 N_i^{(3)} + \ldots\ldots\ldots\ldots \\ V_{ix} &= \varepsilon V_{ix}^{(1)} + \varepsilon^2 V_{ix}^{(2)} + \varepsilon^3 V_{ix}^{(3)} + \ldots\ldots\ldots\ldots \\ V_{iy,iz} &= \varepsilon^{\frac{3}{2}} V_{iy,iz}^{(1)} + \varepsilon^2 V_{iy,iz}^{(2)} + \varepsilon^{\frac{5}{2}} V_{iy,iz}^{(3)} + \ldots\ldots\ldots\ldots \\ \phi &= \varepsilon\phi^{(1)} + \varepsilon^2\phi^{(2)} + \varepsilon^3\phi^{(3)} + \ldots\ldots\ldots\ldots \end{aligned}\right\} \tag{11}$$

Substituting the proposed coordinates and dependent parameters from (10) to (11) through (7) to (9) and equating the appeared lowest power of ε, we get

$$V_{ix}^{(1)} = \phi^{(1)}/\lambda, \quad V_{iy}^{(1)} = I_x/\Omega_i \frac{\partial\phi}{\partial\xi}, \\ V_{iz}^{(1)} = I_x/\Omega_i \frac{\partial\phi}{\partial\xi} \\ N_i^{(1)} = \phi^{(1)}/\lambda^2, \quad N_e^{(1)} = \alpha_1\phi^{(1)} \tag{12a}$$

where $\alpha_1 = \frac{3}{2}\left\{\frac{\eta}{2}(1+T^2) + (1-\eta)^{\frac{1}{2}} - \frac{T^2}{3}(1-\eta)^{-\frac{3}{2}}\right\}$,

And also, we have the following the dispersion relation:

$$\lambda^2 = \frac{1}{\alpha_1(1-\mu_n)} \tag{12b}$$

Similarly, equating the next highest coefficient of ε, i.e. $\varepsilon^{3/2}$ from the respective three directions, viz. x, y, and z of (7) to (9), we get

$$\frac{\partial N_i^{(1)}}{\partial\tau} - M\frac{\partial N_i^{(2)}}{\partial\xi} + \sum_{l=x,y,z} I_l \frac{\partial}{\partial\xi} V_{il}^{(2)} = 0 \tag{13}$$

$$\frac{\partial V_{ix}^{(2)}}{\partial\xi} = \frac{1}{\lambda}\frac{\partial V_{ix}^{(1)}}{\partial\tau} + \frac{I_x}{\lambda}V_{ix}^{(1)}\frac{\partial V_{ix}^{(1)}}{\partial\xi} + \frac{I_x}{\lambda}\frac{\partial\phi^{(2)}}{\partial\xi}, \tag{14}$$

$$\frac{\partial V_{iy}^{(2)}}{\partial\xi} = \frac{\lambda I_x}{\Omega_i^2}\frac{\partial^3\phi^{(1)}}{\partial\xi^3} \,\&\, \frac{\partial V_{iz}^{(2)}}{\partial\xi} = \frac{\lambda I_x}{\Omega_i^2}\frac{\partial^3\phi^{(1)}}{\partial\xi^3} \tag{15}$$

$$I_x^2\frac{\partial^3\phi^{(1)}}{\partial\xi^3} = \mu_e\frac{\partial}{\partial\xi}N_e^{(2)} - \frac{\partial}{\partial\xi}N_i^{(2)} \tag{16}$$

Now, performing some mathematical calculations through (13) to (16) along with (12) and (12b), the final Z–K equation is described as

$$\frac{\partial\phi^{(1)}}{\partial\tau} + A\phi^{(1)}\frac{\partial\phi^{(1)}}{\partial\xi} + B\frac{\partial^3\phi^{(1)}}{\partial\xi^3} \\ + C\frac{\partial}{\partial\xi}\left(\frac{\partial^2\phi^{(1)}}{\partial\eta^2} + \frac{\partial^2\phi^{(1)}}{\partial\zeta^2}\right) = 0 \tag{17}$$

where $A = \frac{q}{p}, B = \frac{1}{p}\,\&\, C = \frac{r}{p}$ with $p = \frac{2}{\lambda^3}, q = \left\{\frac{3}{\lambda^4} - \mu_e\alpha_2\right\}, r = \left(1 + \frac{1}{\Omega_i^2}\right)$,

$$\alpha_2 = \frac{3}{8}\left\{-\frac{\eta}{2}\left(1+5T^2\right) + (1-\eta)^{-\frac{1}{2}} + T^2(1-\eta)^{-\frac{5}{2}}\right\}$$

There are various methods such as (G′/G) expansion method, sech method, sine–cosine method, sine-Gordon method, tanh–coth method, Hirota's direct method, and Lie symmetry approach [60–69] for solving nonlinear partial differential (17) of the type used in the present article. However, we are using tanh method particularly, which falls amongst one of the methods widely accepted by the scientific community throughout the world. Now, to solve the Z–K (17), we have used the transformation $\chi = \gamma(l\xi + m\eta + n\zeta - U\tau)$ and considering $\phi^{(1)}(\xi,\eta,\zeta,\tau) = \psi(\chi)$, which gives

$$-U\psi + \frac{Al}{2}\psi^2 + \gamma^2 l\left(Bl^2 + C\left(m^2+n^2\right)\right)\frac{\mathrm{d}^2\psi}{\mathrm{d}\chi^2} = 0 \tag{18}$$

To derive the required solution of Z–K (17), we used the well-known tanh method [70–72], and for that the transformation, $z = \tanh(\chi)$ and $\psi(\chi) = W(z)$ are introduced, and then (18) becomes

$$-UW + \frac{Al}{2}W^2 + \gamma^2 l\left(Bl^2 + C\left(m^2+n^2\right)\right) \\ \left(\left(1-z^2\right)^2\frac{\mathrm{d}^2W}{\mathrm{d}z^2} - 2z\left(1-z^2\right)\frac{\mathrm{d}W}{\mathrm{d}z}\right) = 0 \tag{19}$$

For finding the series solution of (19), we substitute $W(z) = \sum_{r=0}^{\infty} a_r z^{\rho+r}$, and for leading order analysis of finite terms gives $r = 2$ and $\rho = 0$, and then the $W(z)$ becomes $W(z) = a_0 + a_1 z + a_2 z^2$. Now, substituting the value of $W(z)$ in (19), $W(z) = a_0 + a_1 z + a_2 z^2 = a_0(1 - z^2)$ where $a_0 = -a_2$ and $a_1 = 0$, we get the stationary solution of Z–K (17) as follows:

$$\phi^{(1)} = \phi_m \sec h^2\left\{\frac{\chi}{w}\right\} \tag{20}$$

where $\phi_m = \frac{3U}{Al}$ and $w = \frac{1}{2}\left[U/l\left(Bl^2 + C\left(m^2 + n^2\right)\right)\right]^{1/2}$ are the amplitude and width of the solitary wave, respectively, where l, m, and n are the direction cosine, and U being the constant phase velocity.

4 Results and Discussion

From the analytical solution governed by (20), we analyse the nature and characteristics of solitary wave propagation under different physical situation. Here, we have considered the charged particle density in the plasma as 10^{26-29} cm^{-3}, ambient magnetic field as $10^{10} \sim 10^{12}$ Gauss, and we find the Fermi temperature for those plasma parameters in the range of $3.6277 \times 10^7 K$ [21, 73–76]. Throughout the entire analytical observation, we have considered helium positive ions due to its abundance in the plasma environment of our interest, and also negative ions are assumed to be SF_6^-.

Now, Figure 1 describes the variation of phase speed with magnetic field–related parameter, i.e. η, at different degenerate temperature, T, at a certain normalised electron density. It is seen that the phase velocity increases simultaneously with magnetic quantisation and temperature, which is obvious. But the rate of increase of phase velocity is more with the increase of degenerate temperature than magnetic quantisation. On the other hand, when both magnetic fields, i.e. η, and degenerate temperature, T, have the highest value, the rate of increase of phase velocity is the highest. This is primarily due to the enhancement in the lighter plasma species in the magnetic field lines due to the better internment of the lightest plasma particles with the highest velocity. Similar is the case with Figure 1b. Here, we have plotted the variation of phase velocity with η and T at a certain normalised negative ion density. But, because of the presence of the heaviest negative ion species, the phase velocity is less compared to Figure 1a.

In Figure 2a, we describe the variation of nonlinearity of the plasma system with quantisation parameter and degenerate temperature at a particular normalised electron density. It is found that the as the value of η increases, the nonlinearity decreases, and simultaneously with the increase in degenerate temperature, the nonlinearity increases. If we analyse the situation carefully, we observe that the increase in η is simply the increase in magnetic field and will force the plasma species to move in the line of magnetic field making the plasma species, especially the lighter plasma species to behave in a tidy way, which will surely make the plasma system less nonlinear. On the other hand, as we know, the increase in degenerate temperature, which is nothing but the thermal velocity, will always enforce the plasma system to be more nonlinear. However, the most interesting outcome of the plot is that nonlinearity decreases with increasing η for lower range of the degenerate temperature values (from the lower black solid curve to the green dot dashed curve), whereas it increases with magnetic quantisation parameter for the higher range of the degenerate temperature values (from the red dotted curve to the orange large dashed curve). The prime reason for this phenomenon, which we believe in, may be due to the fact that when the temperature is higher, i.e. the thermal velocity is higher, the faster particles get easily confined, and due to the availability

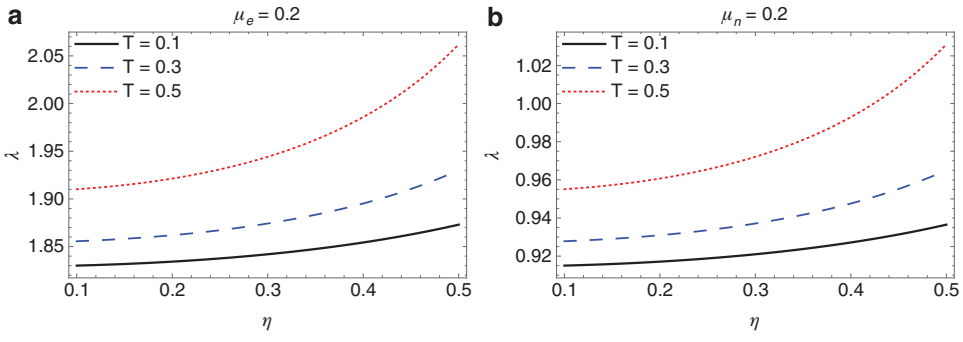

Figure 1: (a) The variation of phase speed with η and degenerate temperature, T at a certain normalised electron density. (b) The variation of phase speed with η and degenerate temperature, T at a certain normalised negative ion density.

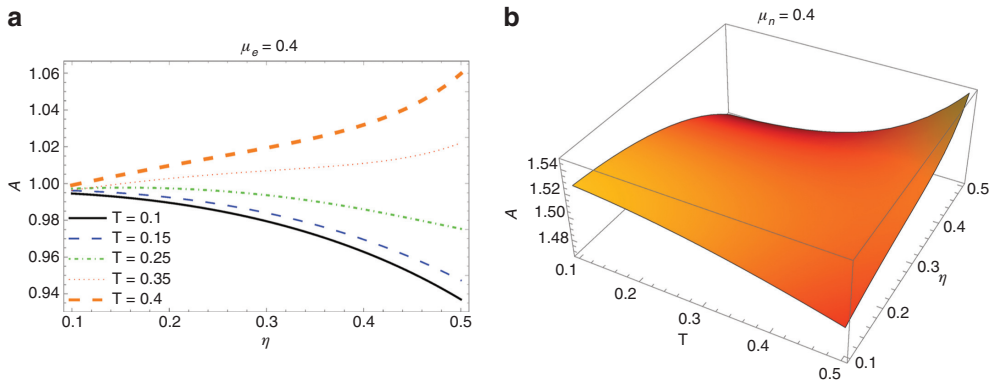

Figure 2: (a) The variation of nonlinearity of the plasma system with quantisation parameter and degenerate temperature at a particular normalised electron density. (b) Variation of nonlinearity with increasing quantisation parameter and degenerate temperature at a particular normalised negative ion concentration.

of such energetic particles along a certain confined path, the frequent and rapid collision probability will increase, which would definitely make the plasma system much more nonlinear. In Figure 2b, we sketch the variation of nonlinearity with increasing quantisation parameter and degenerate temperature at a particular normalised negative ion concentration. As seen in the figure, with increasing degenerate temperature, the nonlinearity decreases, whereas with increasing η, the nonlinearity of the plasma system, increases, which is very interesting. On careful observation, we find the possible reason for this peculiar behaviour due to the presence of enough heavy negative ions. If we analyse the situation, we find that as the degenerate temperature increases, the lighter plasma species, i.e. the degenerate electrons, become more and more faster and as a result are not able to interact with background heavy negative ions because of the such huge difference of mass and as a result also time scale, forcing the system to behave less nonlinearly. On the other hand, with increase in magnetic quantisation, the lighter plasma species, getting more and more efficiently confined along the magnetic field, can now undergo frequent interaction with the background heavy negative ions, making the system more nonlinear. This is absolutely justified if we analyse the figure from a different angle. At a very low value of degenerate temperature (say $T = 0.1$), the nonlinearity decreases with increasing η, which is absolutely similar to the case as described in Figure 2a. The reason behind this phenomenon is that, as the magnetic quantisation or otherwise magnetic field increases, as discussed before, due to streamlined behaviour of the lightest species, the nonlinearity decreases, or otherwise lesser amount of lightest species moving in a conduit way, is available to interact with the random heaviest species and thus restricting the plasma system to behave in a less nonlinear way. This is well justified by the increase in nonlinearity with simultaneous increase in magnetic quantisation and degenerate temperature. This is because as the thermal velocity increases in the presence of magnetic quantisation, the faster particles have greater tendency to be magnetised easily along the applied magnetic field, and as more and more faster particles are available to interact with heavy negative ions, there is a concrete possibility that it will eventually bring more nonlinearity to the plasma system.

In Figure 3, we try to observe the typical trend of the maximum height and width of the solitary wave at different plasma condition with magnetic field. This is very interesting as in some previous work it was reported that the amplitude of the solitary wave is unaffected by the magnetic field and only width is affected. Surprisingly, in such degenerate plasma, the magnetic field has a hefty control of the height of the solitary wave. As seen in Figure 3a, with increasing magnetic field, the maximum amplitude of the solitary wave increases. It is to be noted that the value of η is in the range of 0.1 to 0.6 (used later on to study the propagation of solitary waves) with the chosen magnetic field values, along with other physical parameters (mentioned above) considered in the present study, as it is evident that the outcome of quantised magnetic field aspects through η. However, the choice of these values is not mandatory as one can land on such values of η by changing the values of magnetic field and degenerate plasma density and temperature. Now, coming back to the figure, it is quite apparent from the solution of the shock wave's dynamical equation that the maximum of the solitary wave amplitude varies inversely with the nonlinearity of plasma medium, and as it is clear from Figure 1a, the nonlinearity decreases with increasing magnetic quantisation (and hence magnetic field), and thus the maximum amplitude has almost a linearly increasing

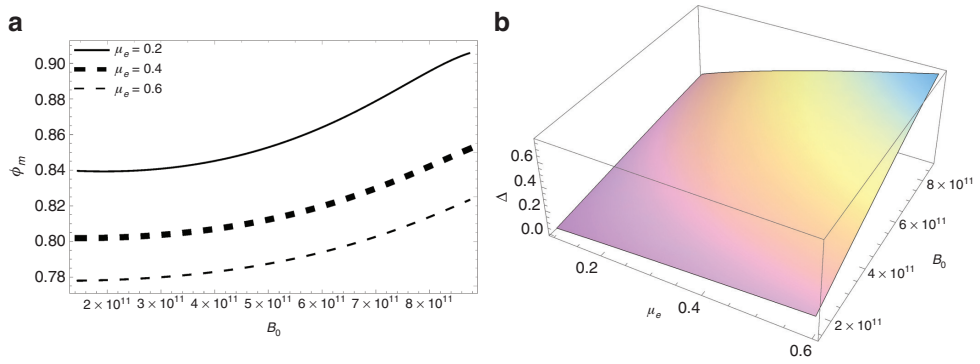

Figure 3: (a) The variation of maximum of solitary wave amplitude with magnetic field and (b) variation of width with magnetic field and normalised electron density.

behaviour with increasing magnetic field as depicted in the figure. Apart from this, the maximum amplitude of the solitary wave decreases with increasing normalised electron density for the same range of magnetic field. The reason may be because as the electron density increases, for obvious reason, the nonlinearity will increase, and hence the maximum amplitude will tend to decrease. However, the width of the solitary wave increases with increasing magnetic field and normalised electron density, and the rate of increase of width with magnetic field is higher than with μ_e, and more importantly, the rate of increase is the highest when both electron density and the magnetic field have the highest within the chosen values. This is because as more and more electrons are available to be channellised by the magnetic field, the width will increase. Moreover, we have seen in Figure 3a and b that the magnetic field has almost the same effect on the height and width of the solitary wave. For example, if we closely observe the figure, it is seen that the percentage rate of increase of amplitude of solitary wave with magnetic field at a particular normalised electron density is similar to the percentage rate of increase of width of the solitary wave with magnetic field at a particular normalised electron density. Figure 4 describes the variation of maximum solitary wave amplitude and width with magnetic field and degenerate temperature. The range of magnetic field is considered the same as before. As seen in Figure 4a, the maximum amplitude decreases with increase in degenerate temperature, which may be due to the rate of increase of the nonlinearity with increasing temperature. On the other hand, on close examination, we find that initially with a small amount of degenerate temperature, the maximum amplitude increases with increasing magnetic field, but as the degenerate temperature increases, the maximum amplitude decreases significantly with increasing magnetic field. This is a very interesting phenomenon. As discussed earlier, the magnetic field will enhance the confinement of the plasma species, and this confinement increases with increasing magnetic field, and also with the increase of temperature, i.e. thermal velocity, the faster particles will be more easily confined in the line of magnetic field. Thus, as more and more faster particles are confined along a channel of magnetic field, due to recurrent and swift interaction amongst themselves and other plasma species, the system starts behaving with higher nonlinearity, and as a result, we can

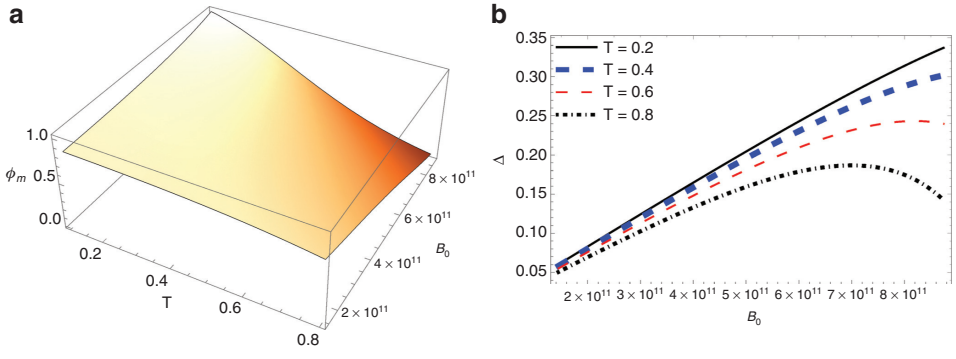

Figure 4: (a) The variation of maximum of solitary wave amplitude with magnetic field and degenerate temperature. (b) Variation of the width with magnetic field at different degenerate temperature.

expect a significant decrease in the maximum amplitude, as it is clear from the above discussion that the maximum amplitude has an inverse relation with nonlinearity in the present study. On the other hand, the width of the solitary wave increases linearly with increasing magnetic field at different degenerate temperature, as seen in Figure 4b. But interestingly, at higher temperature, although initially the width increases linearly with increasing magnetic field, at higher magnetic field, the width tends to show a decrease in its value. This may be because as both temperature and magnetic field increase, there is a possibility that the faster particles can get trapped along the magnetic field lines easily, making the wave less dispersive, and hence we see a lessening value of width at high temperature and high magnetic field.

Figure 5a and b describe the variation of solitary wave potential with magnetic quantisation parameter, analysed based on steady-state solution of the governing equation. As seen in both figures, the height and width of the solitary wave increase in equal proportion with increasing normalised electron density at different increasing values of η. This is in exact accordance with the variation of nonlinearity with increasing magnetic quantisation, as well as with the variation of maximum amplitude and width of the solitary wave with magnetic field, and can be understood in similar context.

In Figure 6a and b, we have shown the variation of solitary wave profile with electron density and negative ion density for a fixed value of temperature. Here, the other plasma parameter such as η is fixed at 0.2. In the figures, we can see that the amplitude declines with increasing normalised electron density, whereas both the amplitude and width get enriched with the enhancement of negative ion density (Figure 6b). This may be because, as the number density of electrons increases, the system will start behaving with higher nonlinearity at such high densities, which will result in a decrease in the amplitude. On the other hand, with negative ions, due to its heavier mass, the interaction with the other plasma species will be less as compared to the electrons, and as its density increases, this interaction will further decrease, which reduces the plasma nonlinearity compared to the electrons, and hence the amplitude increases for the increase in the individual value of negative ion density. But on close examination of both the figures, the absolute value of the shock wave potential is more in the case involving electron (Figure 6a) than negative ion (Figure 6b), which may be due to the heavier negative ions. This is justified by the fact that negative ions increase the width, because as negative ions increase, and accumulates, it will be less dispersive due to its heavy mass, and hence the width increases accordingly.

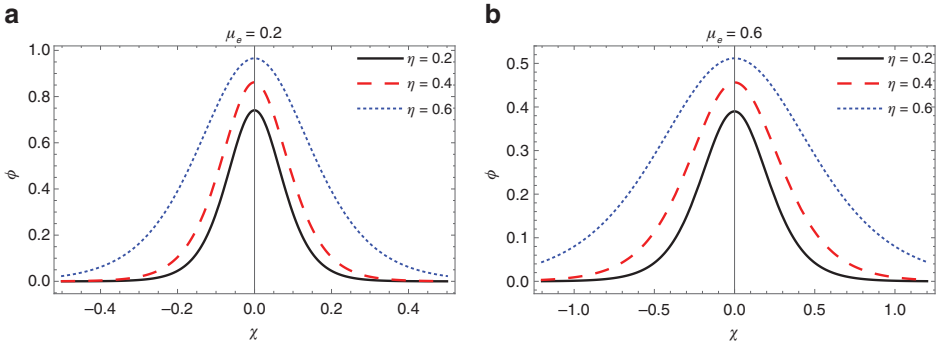

Figure 5: The variation of solitary wave potential with magnetic quantisation parameter at two different normalised electron densities.

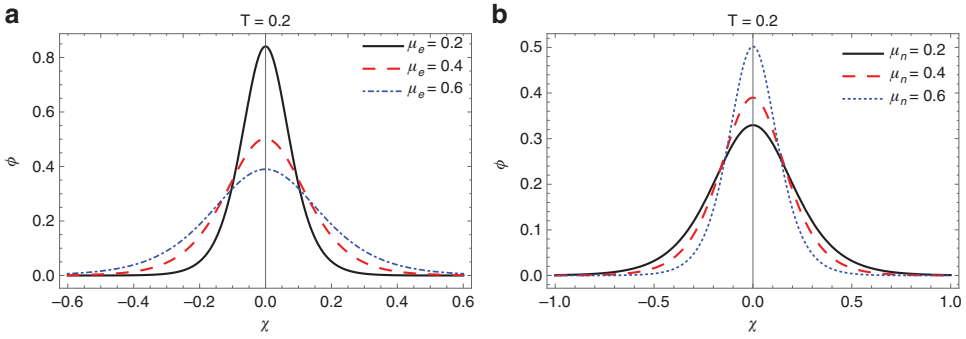

Figure 6: The variation of solitary wave profile with electron density and negative ion density for a fixed value of temperature.

In Figure 7, we plot the variation of the maximum amplitude and width of the solitary wave with normalised heavy negative ion density and degenerate temperature at two different magnetic field or magnetic quantisation parameters. Here, the upper panel (Figure 7a and b) represents the variation of maximum amplitude, whereas the lower panel (Figure 7c and d) represents the variation of width of the solitary wave for the chosen range of the plasma parameter. As seen in Figure 7a, for a lower magnetic field, the maximum amplitude of the solitary wave decreases rapidly at higher values of degenerate temperature and negative ion concentration. However, at lower value of degenerate temperature, the maximum amplitude surged up with negative ion concentration. This is exactly in agreement with the variation of nonlinearity as described in Figure 2b. At higher concentration of negative ion as well as with higher thermal velocity of the lighter species, in the presence of quantised magnetic field, the possibility of frequent interaction increases, as we know that the faster particles will be confined more easily and hence nonlinearity increases, and hence we see a reduction in the maximum value of solitary wave potential. On the other hand, when the negative ion concentration increases continuously, due to its heavy mass, it will lower the phase velocity significantly, and hence a very less probability of interaction with the lighter species when the thermal velocity of the lighter species is less, and in turn, it makes the plasma system less nonlinear due to which the amplitude of the solitary wave increases. On the other hand, when we look at Figure 7b, we see that at lower temperature the height of the solitary wave increases with increase in η, whereas the solitary wave potential decreases when both the η and T increase significantly. This can be understood in the similar context of the explanation of Figure 2b. We have checked the individual values of ϕ_m when $T = 0.8$ and $\mu_n = 0.8$ for $\eta = 0.2$ and $\eta = 0.6$, respectively, and the values come out to be 0.339156 and 0.05195, respectively. The reason behind this drastic decrease in the amplitude can be attributed to few interesting facts. The higher the magnetic field, the higher will be

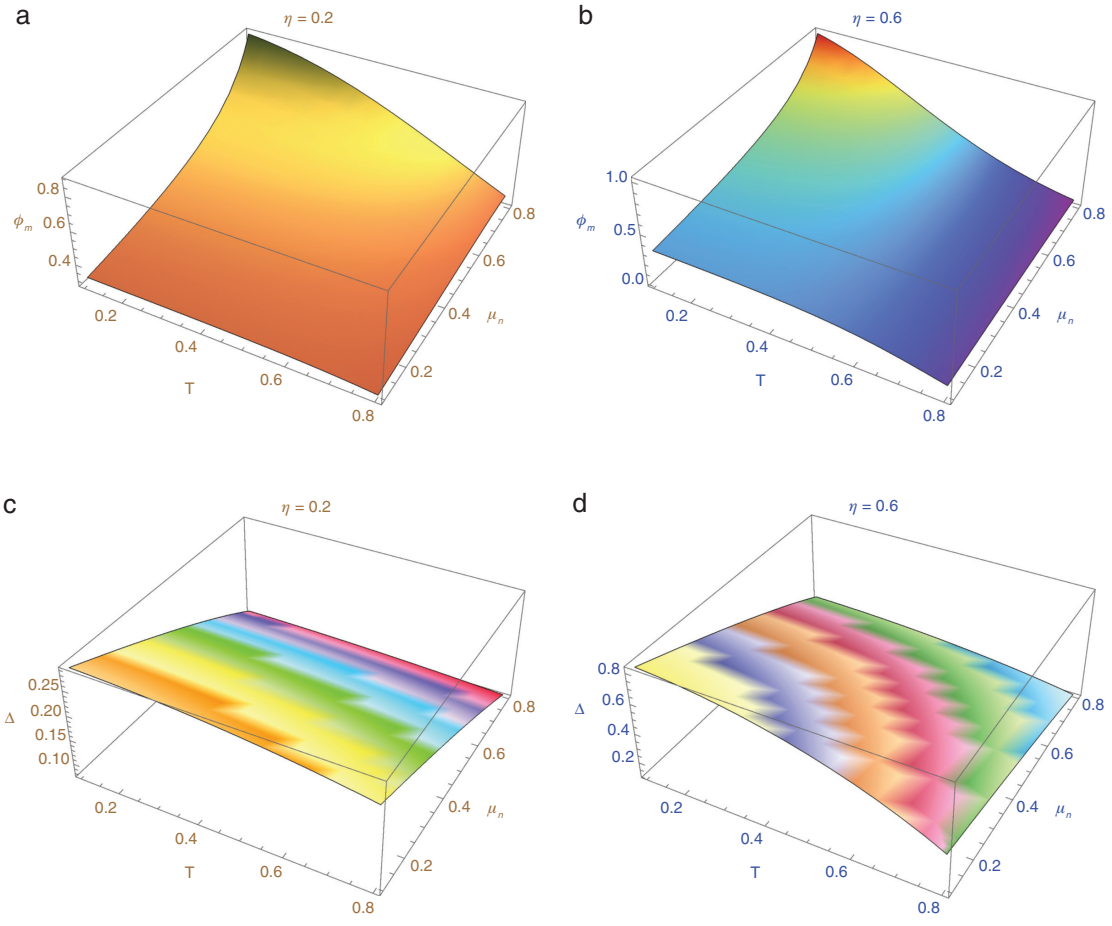

Figure 7: (a and b) Variation of the maximum amplitude with degenerate temperature and normalised negative ion density at two different quantisation parameters η and (c and d) variation of width of the solitary wave with degenerate temperature and normalised negative ion density at two different quantisation parameters η.

the confinement of the lighter plasma species, and if at this point the thermal velocity of the plasma species increases, the lighter particles will become faster, and we know that the faster the particle is, the easier is to be trapped along the magnetic field, and if at this condition negative ion density increases, the amount of interaction will be higher amongst the plasma species, which will evoke higher nonlinearity, and hence we see such a drastic drop in the value of the solitary wave potential when the magnetic quantisation increases significantly. Contrary to this, the width of the solitary wave decreases with the increase of the degenerate temperature and negative ion concentration at the two different magnetic quantisation values considered. However, the rate of decrease of width with degenerate temperature is more when the magnetic quantisation is higher. This is because, first, due to higher magnetic field (with increasing η), the plasma particles will be confined easily; second, due to increase in T, the faster particles will be confined along magnetic field with more ease, which over all would make the plasma system less dispersive (due to better confinement) and hence a decrease in width.

5 Conclusion

The features of solitary wave in a Landau-quantised magnetised quantum plasma in the presence of heavy stationary negative ion are studied. Following the reductive perturbation scheme, Z–K type equation suitable to study such plasma environment is derived. With the help of steady-state solution of the Z–K equation, the effect of various degenerate plasma parameters on the solitary wave propagation is studied. Unlike some previous report, besides its effect on the dispersion of the solitary wave, the magnetic field has a substantial control of solitary wave amplitude also. For a low value of degenerate temperature, the maximum amplitude increases with increasing magnetic field, but as the degenerate temperature increases, the maximum amplitude decreases significantly with increasing magnetic field. The solitary wave is found to be less dispersive at higher temperature and magnetic field, due to the possibility that the faster particles can get trapped along the magnetic field lines easily, making the wave less dispersive, and hence we see lessening value of width at high temperature and high magnetic field. The amplitude (width) decreases (increases) with increasing normalised electron density at a particular degenerate temperature, whereas as the amplitude decreases further with increasing temperature, the width increases further with increasing degenerate temperature. The result described here can be of great importance where such plasma is inevitable, the details of which have been described in the introduction part.

Acknowledgement: The grant received (YSS/2015/001896) by Manoj Kumar Deka from DST-SERB as financial assistance for the current research work is highly appreciated.

Appendix

Derivation of the expression for trapped electron density in a Landau-quantised degenerate plasma.

Following the Fermi–Dirac statistics, the electron occupancy in energy range ε and $\varepsilon + d\varepsilon$, in presence of quantised magnetic field can be written as [45, 52]

$$n_e = \frac{p_{Fe}^2 \eta}{2\pi^2 \hbar^3} \sqrt{\frac{m_e}{2}} \sum_{l=0}^{\infty} \int_0^{\infty} \frac{\varepsilon^{-1/2}}{1 + \exp\big((\varepsilon - U)/T'\big)} \mathrm{d}\varepsilon \quad (1)$$

where $U = e\varphi + \mu - l\hbar\omega_{ce}$ and $\eta = \hbar\omega_{ce}/\varepsilon_{Fe}$; the effect of quantising magnetic field appears through η. The summation above is over all the Landau levels, and we note here $l = 0$ refers to the case without a quantising magnetic field. Now, from basic quantum mechanics of macroscopic system, we know that there is an extremely high density of energy levels in the energy eigenvalue spectrum. The number of levels in a finite range of energy spectrum increases exponentially with the number of particles (N) in the system, and the separation between the levels is proportional to $10^{-\mathrm{N}}$ [53]. Therefore, we can conclude that it is reasonable to take a continuous energy spectrum instead of a discrete one. Thus, to obtain an expression of the density $\mathrm{n_e}$ after integration, we can separate the $l = 0$ case from the summation and replace the summation in (1) by integration, which is obtained from the condition that the integrand must remain a real quantity.

Let $I = \int_0^{\infty} \frac{\varepsilon^{-\frac{1}{2}}}{1+\exp((\varepsilon-U)/T')} \mathrm{d}\varepsilon$, substituting $\frac{\varepsilon-U}{T'} = z$, i.e. $\varepsilon - U = T'z$ and transforming

$$\begin{aligned} I &= \int_0^{\infty} \frac{\varepsilon^{-\frac{1}{2}}}{1 + \exp\left(\frac{\varepsilon-U}{T'}\right)} \mathrm{d}\varepsilon \\ &= T' \int_{-U/T}^{\infty} \frac{(U + T'z)^{-\frac{1}{2}}}{1 + \exp(z)} \mathrm{d}z \\ &= T' \int_0^{U/T} \frac{(U - T'z)^{-\frac{1}{2}}}{1 + \exp(-z)} \mathrm{d}z + T' \int_0^{\infty} \frac{(U + T'z)^{-\frac{1}{2}}}{1 + \exp(z)} \mathrm{d}z \quad (2) \end{aligned}$$

Here $1/(1+\exp(-z))$ can be taken to be equivalent to $\left(1-\frac{1}{e^z+1}\right)$; thus, the above integral (2) becomes

$$I = T\left[\int_0^{U/T'} (U-T'z)^{-\frac{1}{2}}\mathrm{d}z - \int_0^{U/T'} \frac{(U-T'z)^{-\frac{1}{2}}}{e^z+1}\mathrm{d}z + \int_0^{\infty} \frac{(U+T'z)^{-\frac{1}{2}}}{e^z+1}\mathrm{d}z\right] \tag{3}$$

In the second integral of (3), the upper limit U/T' can be replaced by ∞ as $U/T' \gg 1$, and also the integral is rapidly convergent, which allows us to neglect the exponentially small terms. Thus,

$$\begin{aligned} I &= T'\left[\int_0^{U/T'} (U-T'z)^{-\frac{1}{2}}\mathrm{d}z - \int_0^{\infty} \frac{(U-T'z)^{-\frac{1}{2}}}{e^z+1}\mathrm{d}z + \int_0^{\infty} \frac{(U+T'z)^{-\frac{1}{2}}}{e^z+1}\mathrm{d}z\right] \\ &= T'\left[\int_0^{U/T'} (U-T'z)^{-\frac{1}{2}}\mathrm{d}z + \int_0^{\infty} \frac{(U+T'z)^{-\frac{1}{2}}}{e^z+1}\mathrm{d}z - \int_0^{\infty} \frac{(U-T'z)^{-\frac{1}{2}}}{e^z+1}\mathrm{d}z\right] \\ I &= T'\int_0^{U/T'} (U-T'z)^{-\frac{1}{2}}\mathrm{d}z + T'\int_0^{\infty} \frac{(U+T'z)^{-\frac{1}{2}} - (U-T'z)^{-\frac{1}{2}}}{e^z+1}\mathrm{d}z \end{aligned} \tag{4}$$

The first integral of (4) is evaluated in a straightforward manner, and the numerator of the second integral is expanded using Taylor series expansion in the power of z, which yield

$$I = T'\int_0^{U/T'} (U-T'z)^{-\frac{1}{2}}\mathrm{d}z + 2T'^2 f'(U)\int_0^{\infty} \frac{z}{e^z+1}\mathrm{d}z + \frac{1}{3}T'^4 f'''()\int_0^{\infty} \frac{z^3}{e^z+1}\mathrm{d}z + \ldots\ldots \tag{5}$$

Substituting the values of the integrals in (5), we get

$$I = 2U^{1/2} + \frac{\pi^2}{6}T'^2 f'(U) + \frac{7\pi^4}{360}T'^4 f'''(U) + \ldots\ldots \tag{6}$$

Again, substituting back, the values of the differential and neglecting the values of higher order derivatives in (6), we finally find the value of the integral as $I = 2U^{1/2} - \frac{\pi^2 T'^2}{12}U^{-3/2}$. Thus, the integral in (1) becomes

$$n_e = \frac{p_{Fe}^2\,\eta}{2\,\pi^2\,\hbar^3}\sqrt{\frac{m_e}{2}}\sum_0^{\infty}\left(2U^{1/2} - \frac{\pi^2 T'^2}{12}U^{-3/2}\right) \tag{7}$$

As mentioned earlier, we separate the $l=0$ case from the summation and replace the summation by integration from $l=1$ to $l=l_{\max}$, i.e. $\sum_1^{l_{\max}} \to \int_1^{l_{\max}} \mathrm{d}l$. Further, as $U = e\,\varphi + \mu - l\,\hbar\,\omega_{ce} = (\phi + 1 - l\,\eta)\,\varepsilon_{Fe}$, we obtain $l_{\max} = \frac{\phi+1}{\eta}$ in order to have the integrand as a real quantity. Thus, (7) becomes

$$\begin{aligned} n_e &= \frac{p_{Fe}^2\,\eta}{2\,\pi^2\,\hbar^3}\sqrt{\frac{m_e}{2}}\left[\left(2U^{1/2} - \frac{\pi^2 T'^2}{12}U^{-3/2}\right)\right]_{l=0} \\ &\quad + \frac{p_{Fe}^2\,\eta}{2\,\pi^2\,\hbar^3}\sqrt{\frac{m_e}{2}}\left[\int_{l=1}^{\frac{\Phi+1}{\eta}}\left(2\,U^{\frac{1}{2}} - \frac{\pi^2 T'^2}{12}\,U^{-\frac{3}{2}}\right)\mathrm{d}l\right] \end{aligned}$$

Substituting the respective values of U for both the cases, we get

$$\begin{aligned} n_e &= \frac{p_{Fe}^2\,\eta}{2\,\pi^2\,\hbar^3}\sqrt{\frac{m_e}{2}}\left\{2(\phi+1)^{1/2}(\varepsilon_{Fe})^{1/2} - \frac{\pi^2 T'^2}{12}(\phi+1)^{-3/2}(\varepsilon_{Fe})^{-3/2}\right\} \\ &\quad + \frac{p_{Fe}^2\,\eta}{2\,\pi^2\,\hbar^3}\sqrt{\frac{m_e}{2}}\int_{l=1}^{\frac{\phi+1}{\eta}}\left[2\{(\phi+1-l\,\eta)\,\varepsilon_{Fe}\}^{1/2} - \frac{\pi^2 T'^2}{12}\{(\phi+1-l\,\eta)\,\varepsilon_{Fe}\}^{-3/2}\right]\mathrm{d}l \\ &= \frac{p_{Fe}^2\,\eta}{2\,\pi^2\,\hbar^3}\sqrt{\frac{m_e}{2}}\left\{2(\phi+1)^{1/2}(\varepsilon_{Fe})^{1/2} - \frac{\pi^2 T'^2}{12}(\phi+1)^{-3/2}(\varepsilon_{Fe})^{-3/2}\right\} \\ &\quad + \frac{p_{Fe}^2\,\eta}{2\,\pi^2\,\hbar^3}\sqrt{\frac{m_e}{2}}\left[2(\varepsilon_{Fe})^{1/2}\int_{l=1}^{\frac{\phi+1}{\eta}}(\phi+1-l\,\eta)^{1/2}\mathrm{d}l - \frac{\pi^2 T'^2}{12}(\varepsilon_{Fe})^{-3/2}\int_1^{\frac{\phi+1}{\eta}}(\phi+1-l\,\eta)^{-3/2}\,\mathrm{d}l\right] \end{aligned} \tag{8}$$

After integrating and rearranging, (8) becomes

$$n_e = \frac{p_{Fe}^2\,\eta}{2\,\pi^2\,\hbar^3}\sqrt{\frac{m_e}{2}}\Bigg[2(\phi+1)^{1/2}(\varepsilon_{Fe})^{1/2} - \frac{\pi^2 T'^2}{12}(\phi+1)^{-3/2}(\varepsilon_{Fe})^{-3/2} + \frac{4}{3}(\varepsilon_{Fe})^{1/2}\frac{(\phi+1-\eta)^{3/2}}{\eta} + \frac{\pi^2 T'^2}{6}(\varepsilon_{Fe})^{-3/2}\frac{(\phi+1-\eta)^{-1/2}}{\eta}\Bigg]$$

Making use of the respective expression for ε_{Fe}, and T' and performing some mathematical jugglery, we finally arrive at

$$n_e = n_{e0}\Bigg[\frac{3\,\eta}{2}(1+\phi)^{\frac{1}{2}} - \frac{\eta\,T^2}{2}(1+\phi)^{-\frac{3}{2}} + (1+\phi-\eta)^{\frac{3}{2}} + T^2(1+\phi-\eta)^{-\frac{1}{2}}\Bigg],$$

$$\text{where } n_{e0}\left(=p_{Fe}^3/3\pi^2\hbar^3\right) \tag{9}$$

In (9), using Taylor series expansion, we get

$$N_e = \frac{n_e}{n_{e0}} = \left\{\begin{array}{l} \frac{3}{2}\eta\left(1+\frac{\phi}{2}-\frac{\phi^2}{8}+\right)+\left\{(1-\eta)^{\frac{3}{2}}+\frac{3\phi}{2}(1-\eta)^{\frac{1}{2}}+\frac{3\phi^2}{8}(1-\eta)^{-\frac{1}{2}}-\right\} \\ -\frac{\eta T^2}{2}\left(1-\frac{3\phi}{2}+\frac{15\phi^2}{8}-\right)+T^2\left\{(1-\eta)^{-\frac{1}{2}}+\frac{\phi}{2}(1-\eta)^{-\frac{3}{2}}+\frac{3\phi^2}{8}(1-\eta)^{-\frac{5}{2}}+\right\} \end{array}\right\}$$

$$N_e = \frac{n_e}{n_{e0}} = \frac{\eta}{2}\left(3-T^2\right)+(1-\eta)^{\frac{3}{2}}+T^2(1-\eta)^{-\frac{1}{2}}+\frac{3}{2}\phi\left\{\frac{\eta}{2}\left(1+T^2\right)+(1-\eta)^{\frac{1}{2}}-\frac{T^2}{3}(1-\eta)^{-\frac{3}{2}}\right\} + \frac{3}{8}\phi^2\left\{-\frac{\eta}{2}\left(1+5T^2\right)+(1-\eta)^{-\frac{1}{2}}+T^2(1-\eta)^{-\frac{5}{2}}\right\}$$

References

[1] H. Amemiya, B. M. Annaratone, and J. E. Allen, Plasma Sources Sci. Technol. **8**, 179 (1999).

[2] P. H. Chaizy, H. Reme, J. A. Sauvaud, C. d'Uston, R. P. Lin, et al., Nature **349**, 393 (1991).

[3] R. A. Gottscho and C. E. Gaebe, IEEE Trans. Plasma Sci. **14**, 92 (1986).

[4] N. C. Adhikary, M. K. Deka and H. Bailung, Phys. Plasmas **16**, 063701 (2009).

[5] M. K. Deka, A. N. Dev, A. P. Misra, and N. C. Adhikary, Phys. Plasmas **25**, 012102 (2018).

[6] E. F. El-Shamy, R. C. Al-Chouikh, A. El-Depsy, and N. S. Al-Wadie, Phys. Plasmas **23**, 122122 (2016).

[7] A. El-Depsy and M. M. Selim, IEEE Trans. Plasma Sci. **44**, 2901 (2016).

[8] A. U. Rahman, S. A. Khan, and A. Qamar, Plasma Sci. Tech. **17**, 12 (2015).

[9] S. K. El-Labany, W. F. El-Taibany, A. E. El-Samahy, A. M. Hafez, and A. Atteya, IEEE Trans. Plasma Sci. **44**, 842 (2016).

[10] K. Aoutou, M. Tribeche, and T. H. Zerguini, Astrophys Space Sci. **340**, 355 (2012).

[11] S. Sadiq, S. Mahmood, Q. Haque, and M. Z. Ali, Astrophy. J. **793**, 27 (2014).

[12] S. G. Tagare, S. V. Singh, R. V. Reddy, and G. S. Lakhina, Nonlinear Proc. Geoph. **11**, 215 (2004).

[13] S. V. Singh, S. Devanandhan, G. S. Lakhina, and R. Bharuthram, Phys. Plasmas **23**, 082310 (2016).

[14] T. Sreeraj, S. V. Singh, and G. S. Lakhina, Phys. Plasmas **25**, 052902 (2018).

[15] R. Rubia, S. V. Singh, and G. S. Lakhina, Phys. Plasmas **25**, 032302 (2018).

[16] R. Rubia, S. V. Singh, and G. S. Lakhina, J. Geophys. Res. Space Phys. **122**, 9134 (2017).

[17] G. S. Lakhina, S. V. Singh, R. Rubia, and T. Sreeraj, Phys. Plasmas **25**, 080501 (2018).

[18] S. Devanandhan, S. V. Singh, G. S. Lakhina, and R. Bharuthram, Commun. Nonlinear Sci. Numer. Simulat. **22**, 1322 (2015).

[19] G. S. Lakhina and S. Singh, in: Kappa Distributions: Theory and Applications in Plasmas (Ed. G. Livadiotis), 1st ed., Elsevier eBook, Oxford OX5 1GB, UK 2017.

[20] M. K. Deka and A. N. Dev, Ann. Phys. **395**, 45 (2018).

[21] J. Landstreet, Phys. Rev. **153**, 1372 (1967).

[22] S. L. Shapiro and S. A. Teukolsky, Black Holes, White Dwarfs, and Neutron Stars, John Wiley and Sons, New York, USA 1981.

[23] V. M. Lipunov, Neutron Star Astrophysics, Nauka, Moscow 1987.

[24] M. J. Iqbal, H. A. Shah, W. Masood, and N. L. Tsintsadze, Eur. Phys. J. D **72**, 192 (2018).

[25] A. A. Mamun and P. K. Shukla, Phys. Plasmas **17**, 104504 (2010).

[26] S. Chandrasekhar, An Introduction to the Study of Stellar Structure, University of Chicago Press, Chicago, IL, USA 1939.

[27] L. K. Ang, T. J. Kwan, and Y. Y. Lau, Phys. Rev. Lett. **91**, 208303 (2003).

[28] T. C. Killian, Nature **441**, 297 (2006).
[29] Y. D. Jung, Phys. Plasmas **8**, 3842 (2001).
[30] M. Opher, L. O. Silva, D. E. Dauger, V. K. Decyk, and J. M. Dawson, Phys. Plasmas **8**, 2454 (2001).
[31] N. L. Tsintsadze, H. A. Shah, M. N. S. Qureshi, and M. N. Tagviashvili, Phys. Plasmas **22**, 022303 (2015).
[32] P. Sumera, A. Rasheed, M. Jamil, M. Siddique, and F. Areeb, Phys. Plasmas **24**, 122107 (2017).
[33] S. Eliezer, P. Norreys, J. T. Mendonça, and K. Lancaster, Phys. Plasmas **12**, 052115 (2005).
[34] U. Wagner, M. Tatarakis, A. Gopal, F. N. Beg, E. L. Clark, et al., Phys. Rev. E **70**, 026401 (2004).
[35] A. Mondal, S. V. Rahul, R. Gopal, D. Rajak, M. Anand, et al., AIP Adv. **9**, 025115 (2019).
[36] M. Irfan, S. Ali, and A. M. Mirza, Phys. Plasmas **24**, 052108 (2017).
[37] M. J. Iqbal, W. Masood, H. A. Shah, and N. L. Tsintsadze, Phys. Plasmas **24**, 014503 (2017).
[38] H. A. Shah, W. Masood, M. N. S. Qureshi, and N. L. Tsintsadze, Phys. Plasmas **18**, 102306 (2011).
[39] A. N. Dev and M. K. Deka, Phys. Plasmas **25**, 072117 (2018).
[40] M. R. Hossen, L. Nahar, S. Sultana, and A. A. Mamun, High Energ. Dens. Phys. **13**, 13 (2014).
[41] S. Mahmood, S. Sadiq, Q. Haque, and M. Z. Ali, Phys. Plasmas **23**, 062308 (2016).
[42] E. F. El-Shamy, R. C. Al-Chouikh, A. El-Depsy and N. S. Al-Wadie, Phys. Plasmas **23**, 122122 (2016).
[43] M. M. Masud and A. A. Mamun, Pramana J. Phys. **81**, 169 (2013).
[44] S. Ghosh, Euro Phys. Lett. **99**, 36002 (2012).
[45] F. Haas and S. Mahmood, Phys. Rev. E **94**, 033212 (2016).
[46] B. Sahu, Physica A **509**, 162 (2018).
[47] M. R. Hossen and A. A. Mamun, Braz J Phys **44**, 673 (2014).
[48] S. Hussain, N. Akhtar, and Saeed-ur-Rehman, Chin. Phys. Lett. **28**, 045202 (2011).
[49] S. Hussain and N. Akhtar, Phys. Plasmas **25**, 062109 (2018).
[50] L. Tie-Lu, W. Yun-Liang, and L. Yan-Zhen, Chin. Phys. B **24**, 025202 (2015).
[51] B. Sahu, B. Pal, S. Poria, and R. Roychoudhury, J. Plasma Phys. **81**, 905810510 (2015).
[52] W. Masood and B. Eliasson, Phys. Plasmas **18**, 034503 (2011).
[53] M. M. Haider, S. Akter, S. S. Duha, and A. A. Mamun, Cent. Eur. J. Phys. **10**, 1168 (2012).
[54] H. A. Shah, M. J. Iqbal, N. Tsintsadze, W. Masood, and M. N. S. Qureshi, Phys. Plasmas **19**, 092304 (2012).
[55] A. Rahman, S. Ali, A. M. Mirza, and A. Qamar, Phys. Plasmas **20**, 042305 (2013).
[56] A. Rahman, W. Masood, B. Eliasson, and A. Qamar, Phys. Plasmas **20**, 092305 (2013).
[57] M. I. Shaukat, Eur. Phys. J. Plus **132**, 210 (2017).
[58] L. D. Landau and E. M. Lifshitz, Statistical Physics, Butterworth-Heinemann, Oxford 1980.
[59] L. Tsintsadze, NAIP Conference Proceedings **1306**, 89 (2010).
[60] M. Mehdipoor, Astrophys Space Sci. **338**, 73 (2012).
[61] P. Kaliappan and M. Lakshmanan, J. Math. Phys. **23**, 3 (1982).
[62] M. Mehdipoor and A. Neirameh, Astrophys Space Sci. **337**, 269 (2012).
[63] M. Musette and R. Conte, Phys. A Math. Gen. **27**, 3895 (1994).
[64] S. Kumar and D. Kumar, Comput. Math. Appl. **77**, 2096 (2019).
[65] D. Kumar and S. Kumar, Comput. Math. Appl. **78**, 857 (2019).
[66] S. Kumar, D. Kumar, and A. M. Wazwaz, Phys. Scr. **94**, 065204 (2019).
[67] M. Guo, H. Dong, J. Liub, and H. Yang, Nonlinear Anal. Model. **24**, 11 (2019).
[68] J. Sarma, Chaos Soliton. Fract. **39**, 277 (2009).
[69] J. Sarma, Chaos Soliton. Fract. **42**, 1599 (2009).
[70] K. Abe and O. Inoue, J. Comput. Phys. **34**, 202 (1980).
[71] A. M. Wazwaz, Comput. Math. Appl. **45**, 1101 (2005).
[72] G. C. Das and J. Sarma, Phys. Plasmas **6**, 4394 (1999).
[73] A. M. Wazwaz, Appl. Math Comput. **202**, 275 (2008).
[74] D. Koester and G. Chanmugam, Rep. Prog. Phys. **53**, 837 (1990).
[75] V. M. Lipunov, Astrophysics of Neutron Stars, Springer-Verlag, Berlin, Germany 1992.
[76] S. S. Ghosh and G. S. Lakhina, Nonlinear Proc. Geoph. **11**, 219 (2004).